Research Article | Vol. 30, No. 21 / 10 Oct 2022 / Optics Express 38152
Optics EXPRESS

Design and transmission analysis of trench-assisted multi-core fibre in standard cladding diameter

XUN MU,* ALESSANDRO OTTINO, FILIPE M. FERREIRA, AND GEORGIOS ZERVAS

Optical Networks Group, Department of Electronic and Electrical Engineering, University College London, London, UK
uceexmu@ucl.ac.uk

Abstract: 6-core and 8-core trench-assisted heterogeneous fibres in standard cladding diameter are designed using artificial intelligence-based techniques including a cut-off wavelength regressor. The designs proposed here, for the first time, suppress crosstalk at 1550 nm of 8-core fibre to as low as −55 dB/km covering the whole S+C+L band while keeping coating loss below 0.001 dB/km. We compare them to reveal the influence of the additional cores in the 125 μm cladding diameter scenario. We report on the transmission characteristics and performance of the MCFs in terms of capacity and spatial spectral efficiency, including the influence of bandwidth, effective mode area, distance and crosstalk, for a range of transmission distances. The artificial intelligence-based method and insights given can be used to significantly speed up and tailor designs for a variety of telecom and datacom applications.

1. Introduction

Multi-core fibre (MCF) design is the first step of developing space division multiplexing (SDM). Uncoupled MCFs in standard cladding diameter attracted plenty of interest recently because they benefit from both low inter-core crosstalk (XT) and compatibility with existing standard single-mode fibre (SSMF) and SMF-based equipment [1–3]. The existing uncoupled MCFs in standard cladding diameter have 4 cores [1,2] to 8 cores [3–6]. In [3], the authors present the only fabricated 8-core fibre supporting only O-band. As for other 8-core fibre designs based only on simulation there are the fibres in [4] designed to support O-band and those in [5] supporting wide-band (cut-off wavelength = 1300 nm) lack the critical analysis of the coating loss - particularly relevant for high-index coating [7]. Based on our estimations, the coating loss of the fibre cores reported range from 0.067 dB/km to 1.15 dB/km which makes them unsuitable. Recently, [6] reported a 8-core fibre design optimised to keep coating loss smaller than 0.01 dB/km but covering only the C-band.

The artificial intelligence (AI)-based automatic method [8] was proposed to design 6-core trench-assisted (TA) MCFs for improving the efficiency and exploring optimal MCF structures for different objectives. Here we further develop the AI-based method by including a cut-off wavelength regressor and exploring TA MCF designs with higher spatial density.

Previous works [5,9,10] reporting the design of TA MCFs ignored the unique loss behaviour of trench-assisted fibre core reported in [11]. Instead, they treated trench-assisted profiles the same as step-index ones, which leads to significant cut-off wavelength miscalculation. To address the shortcoming of the prior art, we used Lumerical to estimate the cut-off wavelength of 10,000 TA fibre core profiles by measuring the TA fibre core's LP11 loss at straight conditions. The data were used to train a machine learning regressor to speed up the design process by around $10^7\times$.

#472430 https://doi.org/10.1364/OE.472430
Journal © 2022 Received 11 Aug 2022; revised 21 Sep 2022; accepted 21 Sep 2022; published 29 Sep 2022

Optics EXPRESS

On the other hand, we report the optimisation of 6-core and 8-core fibres cover C+L- and S+C+L- bands under coating loss constraint — smaller than 0.001 dB/km while optimising the inter-core XT or effective mode area (A_{eff}). Inter-core XT is one of the key metrics in the design of weakly-coupled MCF. When the spatial density is increased, the core pitch is reduced leading to higher inter-core XT. However, for a given pitch, it has been shown that inter-core XT can be reduced by making neighbour cores heterogeneous [12]. Therefore, the assumption of the fibre is that there are two types of cores neighboring to each other for controlling XT level. On the other hand, A_{eff} influences the nonlinear interference (NIL) noise in transmission and it is a performance metrics of MCF when compared to the SSMF.

Moreover, following the optimum fibre designs process, their capacity is evaluated. Transmission performance for distances between 50 km to 10000 km is obtained utilising a Gaussian noise (GN) model. Given the ultra-wide-bandwidth of the designs proposed, the transmission model includes inter-channel stimulated Raman scattering (ISRS) [13]. The relationships between capacity and the optical properties (bandwidth, A_{eff} and XT) of the MCFs are thoroughly analysed. The influence brought by adding two more cores into the standard cladding diameter on the fibre core structures and the optical properties are investigated. It can be noted that:

- The search area of the MCF designs can be reduced according to the optimised designs. In particular, the total permutation number reduces by 991× for 6-core case and 3.6e5× for 8-core case.
- The 8-core fibres offer 32% more (approaching the theoretical 33.3%) capacity than the 6-core fibre at 50 km transmission while covering the CL band or SCL band. At 10000 km, the 8-core fibres still offer higher capacity than 6-core fibres but only by 7% due to higher XT.
- The XT-induced capacity penalty increases super-linearly with XT. Meanwhile, the capacity penalty curve becomes sharper for longer transmission length.
- A_{eff} increase brings similar benefits to the capacity of 6-core and 8-core fibres.

2. Design methodology

This work assumes that there are two types of cores alternated in a ring — the effective index difference between neighbor cores reduces the inter-core XT. The schematic diagram of the 8-core TA fibre design optimised here is illustrated in Fig. 1. Core pitch of 32.5 μm for 6-core fibres and 24.87 μm for 8-core fibres respectively, outer cladding thickness (OCT) of 30 μm (for reducing coating loss) [14] and cladding diameter of 125 μm are set in the fibre design. Assuming the outer and inner cladding as pure silica, each core has 5 refractive-index profile parameters which can be optimised. Hence, for each fibre, there are 10 variables to be optimised in total (5 per core type). The parameters are limited to the manufacturing precision shown in Table 1. a_1, w_{cl} and w_{tr} denote core radius, inner cladding width and trench width, respectively. Δ_1 and Δ_2 are the relative refractive-index difference between core and cladding, trench and cladding, respectively.

In the PSO algorithm [15], each particle contains these 10 variables which represent a MCF structure. The particles search the optimal fibre structure according to their corresponding fitness values. In the fitness value calculation, the overlap condition and the coating loss condition are checked as the first step for all the optimisations:

- Overlap condition: the distance between the adjacent trench edges must be ≥ 2 μm for preventing superposition;
- Coating loss condition: the coating loss must be ≤ 0.001 dB/km.

Optics EXPRESS

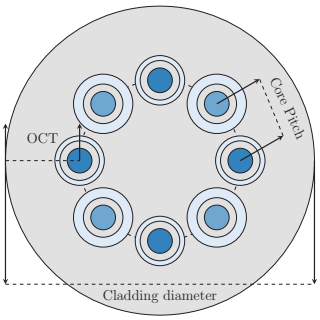

Fig. 1. Hete-TA-MCF layout; (OCT: outer cladding thickness.)

Table 1. Index parameters.

Parameters	Range	Step	Choices
a_1 [μm]	4 ~ 6	0.1	21
w_{cl} [μm]	2.5 ~ 7.5	0.1	51
w_{tr} [μm]	2.5 ~ 7.5	0.1	51
Δ_1	0.3% ~ 0.6%	0.01%	31
Δ_2	−0.7% ~ −0.35%	0.01%	36

If and only if both conditions are satisfied, the fitness values are calculated based on two different objectives: maximise-A_{eff} (A_{eff}-*optimization*) or minimise-XT while constraining A_{eff} (*XT-optimization*). Exploring two objectives is key to the whole design process as the performance of meta-heuristics and in turn the generated fibre structure significantly relies on the analytical formulation of the objective functions. The two types of cores have different A_{eff} since MCF is heterogeneous. Herein we explore the maximum of the average A_{eff} of the two types of cores.

2.1. Cut-off wavelength regression

The TA fibre core has different loss mechanism comparing to the step-index cores [11]. Since TA fibre core is insensitive to bending, its bending loss is not significant around cut-off wavelength. Instead the leakage loss of LP11 mode determines the cut-off wavelength. Thus, in this work a regressor of cut-off wavelength is trained based the loss of the LP11 mode when the fibre is in straight condition. The five parameters in Table 1 are the inputs of the regressor. The data is collected with Finite Difference Eigenmode (FDE) solver in Lumerical. A dataset of 10k core profiles and their associated cut-off wavelengths is utilised in the regressor training as shown in Fig. 10(a) in Appendix A. In data pre-processing, it is found that there is high correlation between each input (each and every parameter of a core profile) and output (cut-off wavelength). Hence, one multivariate linear regressor is trained for presenting the linear relationships among inputs and output. Then, the other multivariate linear regressor is trained for the linear relationships between any of the multiplications of feature pairs and the first-order residual. At the end, the second-order residuals of the data is used to train a XGBoost regressor. The workflows used to create cut-off wavelength regressors and to predict the cut-off wavelength are illustrated in Fig. 10 in Appendix A. After the hyper-parameter optimisation, the regressors are proven to predict the cut-off wavelength with an absolute error of 14.93 nm to be the 99% cumulative density function (cdf) in Fig. 2. Therefore, in the MCF optimisation, the cut-off wavelength criterion is set to be (1530 − 14.93) nm for CL-band fibre and (1460 − 14.93) nm for SCL-band fibre. The regressors inference time on Nvidia A100 GPU is 2.45 μs for single calculation. The regressors are 10^7 times faster compared to estimation time using Lumerical FDE solver,.

Optics EXPRESS

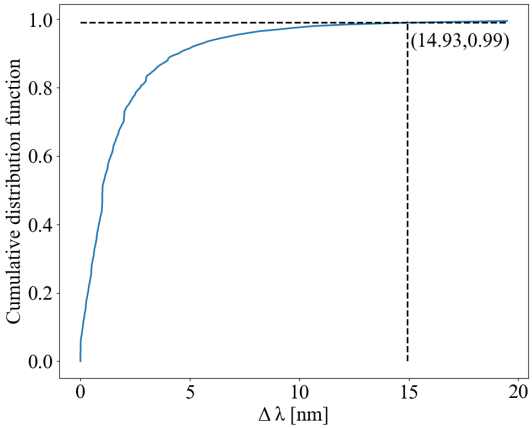

Fig. 2. Cumulative density function of cut-off wavelength regressors increases with absolute error range.

2.2. *Constrains combinations*

The design process starts with the most challenging widest bandwidth requirement using the maximise-A_{eff} objective. The process to go through the constrain combinations of 8-core fibres are illustrated in Fig. 3 as example. The PSO cannot find solutions satisfying all the constrains for the first two cases—OESCL band and ESCL band. That means that an 8-core fibre cannot be designed to support OESCL or ESCL bands. The design process moves to SCL band bandwidth requirement. The maximum average A_{eff} is found to be 60.28 μm^2. Following this, the design process carries on with the second objective function that aims to the minimise-XT while constraining the A_{eff} of the two types of cores within [60 70] range. Again, it is impossible to find solution in which the A_{eff} is above 60 for both types of cores simultaneously. Then, the A_{eff} constraint is reduced to [55 65] and [50 60]. The design process is repeated under the CL bandwidth constraint.

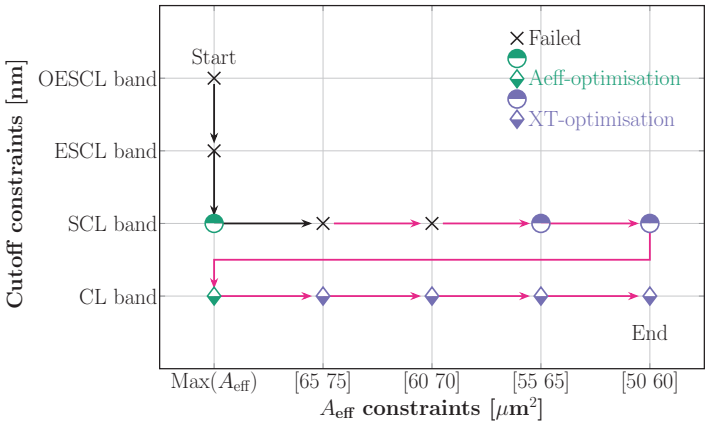

Fig. 3. Optimisation process to go through combinations of constraints taking 8-core fibre as example. The green marks are for *A_{eff}-optimisation* and the blue marks are for *XT-optimisation*. The circle marks represent the SCL band fibres and the diamond marks stand for the CL band fibres. The representation of mark color and shape to the optical band are valid for all the following figures.

Optics EXPRESS

In 6-core fibre case, the maximum average A_{eff} is found to be 64.41 μm^2 for SCL band and 73.65 μm^2 for CL band. Fibres are designed in XT-optimisation for SCL band for A_{eff} from [70 80] to [50 60] and for CL band for A_{eff} of [60 70] and [55 65]. The details about designing the objective functions including all the constraints is shown in [15].

Particles optimise the MCF structure based on the fitness value. For each design point, there are only up to 10^6 evaluations to converge which is nine orders of magnitude less than the brute force method ($\sim 10^{15}$). Then, the optimised MCF structure is extracted for each constraints combination. The flowchart, Fig. 13 in Appendix D, shows the PSO process.

3. Fibre design analysis

After going through all the combinations of cut-off wavelength and A_{eff} constrains, 9 designs of 6-core fibres and 8 designs of 8-core fibres are obtained. Solid and half marks are used to represent 6-core fibres and 8-core fibres respectively.

The optimised fibres are compared to MCFs previously presented in the literature [1,15–18], with standard cladding diameter, in terms of XT and relative core multiplicity factor (RCMF) [15]. RCMF is most useful to understand how the A_{eff} of cores in the MCF is against a SSMF and to make comparison among MCFs with different core numbers.

6-core fibres in XT-optimisation have ultra-low XT less than −80 dB/km while the two designs in A_{eff}-optimisation have XT around −60 dB/km which is more than 20 dB/km higher. That is due to both their higher RCMFs and the homogeneous structures. Our 6-core fibres have RCMF from 4.23 to 5.52. Compared to the reference fibres shown as black square marks, the A_{eff}-optimisation 6-core fibres have up to 1.25 higher RCMF than the 4- and 5- core fibres [1,18] while more than 5 dB lower XT than the 6-core fibre [16].

The 8-core fibres have higher core density, which generally leads to higher XT. Most of them are between −45 dB/km and −60 dB/km except for the two results of A_{eff}-optimisation and the [65 75] case for CL band. The two in A_{eff}-optimisation are heterogeneous but their high RCMFs result in high XT. As for the latter one, it has similar RCMF to that of the A_{eff}-optimisation but homogeneous structure. Thus, it holds the highest XT. Compared to the 6-core [16] and 7-core [17] fibres in Fig. 4, it can be seen that most of our 8-core fibre designs have similar XT, even smaller XT. Meanwhile, the new 8-core fibres have comparable RCMFs to that of the 6-core and 7-core fibres — between 5.42 and 6.50. As for 8-core fibre in [6], its A_{eff} is 80 μm^2 (the corresponding RCMF is 8), however, it has a higher XT than −30 dB/km, which is not suitable for long-haul transmission. Compared to it, our 8-core fibres have up to 35 dB lower XT.

To explore the fibre structures' difference between two core numbers, the refractive-index profile parameters' range in the final designs are illustrated in Fig. 5. The search area is reduced apparently. The total permutation number reduces by 991× for 6-core case and 3.6e5× for 8-core case. The permutation number is reduced more for 8-core fibres because the compact fibre structure limits the fibre structure.

a_1 and Δ_1 play the role of meeting the constraints of cut-off wavelength and A_{eff}. In both cases, the range of them can be reduced to half width. In the 6-core fibre designs, w_{tr} converges to a very narrow region close to the widest while w_{cl} lays at the narrow side. In the 8-core fibres, although the trench is the deepest, the w_{tr} operates within a broader range because of the smaller core pitch and the overlap condition. w_{cl} converges to the narrowest layer width. Compared to the 6-core fibres, Δ_1 of the 8-core fibres is slightly higher. With the narrower w_{tr}, fibre cores need higher index difference to compensate the light confinement for preventing exceeding coating loss constraint. The key conclusion here is that the trench can be fixed to be deep While having the small w_{cl}. Should there be ample space/core-pitch, the trench can also be fixed to the widest. This can simplify and speed-up the MCF design by just optimising the a_1 and Δ_1. This can be particularly valuable when designing MCFs with large core number across larger cross-sectional area.

Optics EXPRESS

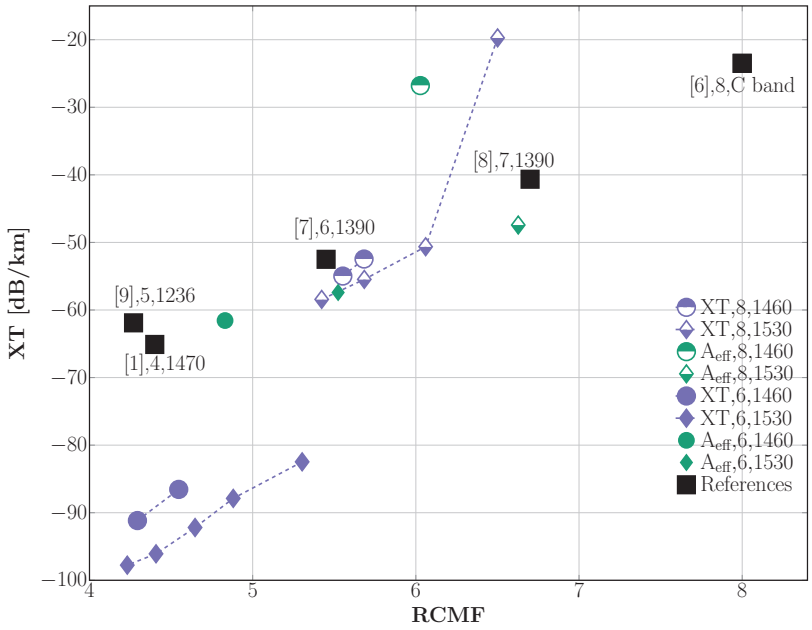

Fig. 4. XT and RCMF of the MCFs. Next to the square marks show the reference, core number and cut-off wavelength in nm. As for the legend, next to the marks show the design objective (XT or A_{eff}), core number (6 or 8) and cut-off wavelength constraint (1460 or 1530).

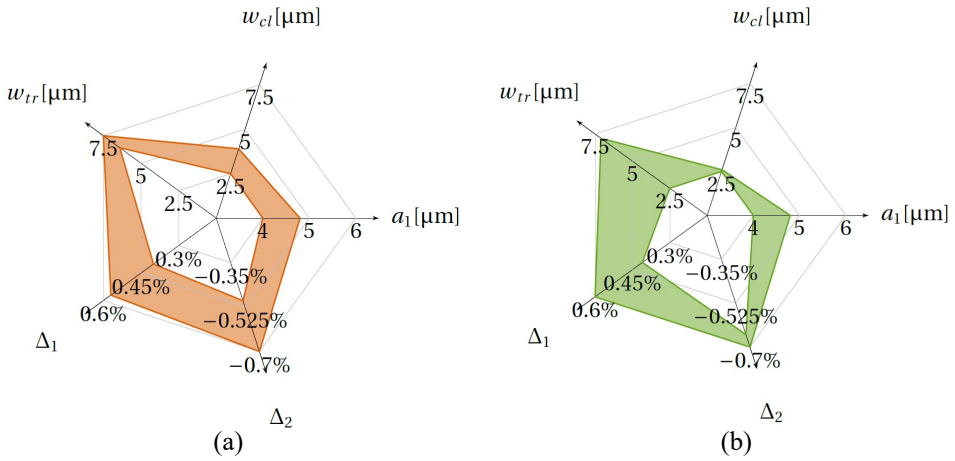

Fig. 5. Refractive-index profile parameters' range of (a) the 6-core fibres and (b) the 8-core fibres.

Optics EXPRESS

4. Transmission performance

We explore the capacity of the MCFs from 50 km to 10000 km transmission length and analyse the effects of the optical properties on the capacity in this section. The capacity of MCF is calculated using the ISRS GN model [13] considering XT as part of the noise [19]:

$$SNR = (SNR_0^{-1} + XT)^{-1}, \tag{1}$$

The calculation assumes Gaussian modulation, uniform launch power −2 dBm/channel, bandwidth 49.5 GHz/channel with 50 GHz channel spacing and 50 km per span. The assumptions on the fibre attenuation and the noise figure (NF) across the spectrum used in the capacity calculation are in Appendix B. The full-band capacity is calculated while considering all the optical bands the MCFs can cover as shown in Fig. 6. We pick the 6-core and 8-core fibre with best capacity for CL- and SCL-band respectively. The properties of these four fibres are shown in Table 2 in Appendix C. Different from the case of the 6-core fibres—the fibres with highest capacity are close to the larger A_{eff} side, the fibre with the lower XT offers the optimum capacity among the 8-core fibres. The influence of A_{eff} and XT on capacity will be elaborated respectively later.

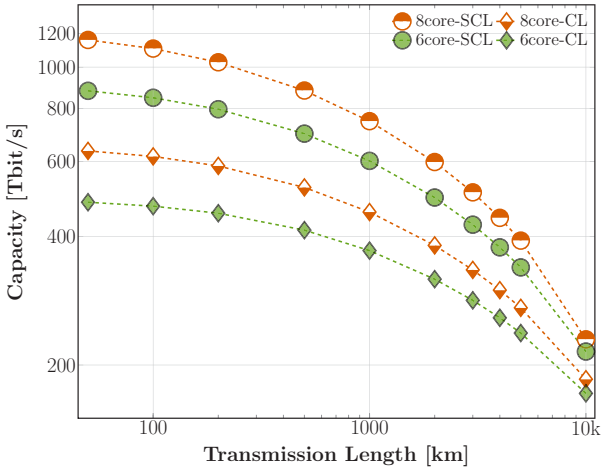

Fig. 6. Capacity of the MCFs for from 50 km to 10000 km transmission

The SCL-band 8-core fibre provides a highest capacity at 50 km (1157.97 Tbit/s) while the SCL-band 6-core fibre delivers 879.71 Tbit/s. The 8-core fibre holds 31.63% higher capacity than the 6-core fibre while in the CL-band case, the 8-core fibre has 31.96% higher capacity. Both are very close to the 33.33% spatial density increase. At 50 km, the influence brought by XT is negligible. The small margin to the ideal case is due to the smaller A_{eff} of the 8-core fibre compared to the 6-core fibre.

As the transmission length increases, the capacity drops because of the accumulated noise. The capacity of 8-core fibres keeps above that of 6-core fibres. The capacity of the 8-core fibre keeps reducing at faster pace than the 6-core fibre since the 8-core fibre has higher XT (27.04 dB for CL-band and 9.1 dB for SCL-band) and smaller A_{eff} (13.87 μm^2 for CL-band and 7.58 μm^2 for SCL-band). At 10000 km, the total capacity of the SCL-band 8-core fibre is 6.82% more compared to the SCL-band 6-core fibre. Meanwhile, the total capacity of the CL-band 8-core fibre is 7.97% more than that of the CL-band 6-core fibre.

In the following discussion, we analyse the influence of the bandwidth, A_{eff} and XT on the transmission performance. Firstly, in order to further investigate the MCF transmission

Optics EXPRESS

performance dependence on the bandwidth, the metric of spatial spectral efficiency is used here in Fig. 7. Spatial spectral efficiency (SSE) is defined as the spectral efficiency per cladding area of the SSMF [20]. Herein since the MCFs are designed in the standard cladding diameter, SSE equals to the spectral efficiency per fibre which is easily compared with the SSMF. There are several factors leading to the spectral efficiency degradation on ultra-wideband optical fibre transmission system:

- The ISRS-induced penalty increases with an increase in the channel number;
- The attenuation is higher out of the C band, especially at short wavelengths;
- The A_{eff} is smaller at the short wavelengths, which brings more non-linearity into the wide-band capacity;
- In the MCF case, the XT increases with longer wavelength;
- The optical components have different performances across the entire bandwidth. For example, the NF in S band is higher than in C band.

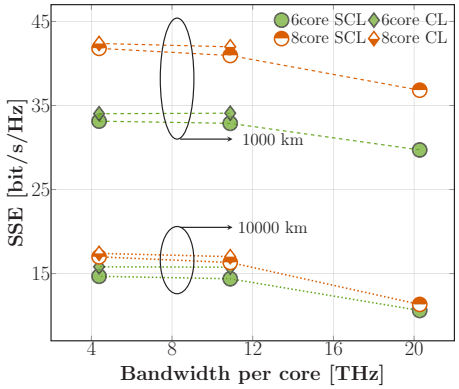

Fig. 7. Spatial spectral efficiency for different bands (C, CL, SCL from left to right) at 1000 km and at 10000 km.

We report on the SSE versus bandwidth per core in Fig. 7 from C band to full band in two transmission lengths, 1000 km and 10000 km. First of all, the SSE keeps almost the same when the operation changes from C band only to CL band. That means that expanding the transmission into CL band would benefit from the wider bandwidth without apparent SSE degradation. At 1000 km, the 8-core fibre has 42.38 bit/s/Hz SSE while operating only in C-band, about 8.36 bit/s/Hz higher than the 6-core fibres. When it comes to 10000 km, the SSE of the 8-core fibre falls by around 34.98 bit/s/Hz while that of the 6-core fibres decreases by about 18.22 bit/s/Hz. Thus, the SSE of 8-core fibre at 10000 km is similar to that of the 6-core fibre.

The SSE of the 8-core fibre decreases faster than that of the 6-core fibres when the bandwidth is increased from CL band to SCL band. The relatively high XT, high attenuation and small A_{eff} of the 8-core fibre lead to this fast drop. This drop makes the SSE of SCL-band 8-core and 6-core fibre more closer, resulting the smaller capacity increase in SCL-band case compared to CL-band case in the total capacity at 10000 km.

Furthermore, the capacity sensitivity on A_{eff} and XT are analysed. Higher A_{eff} corresponds to lower nonlinear effects, which leads to higher capacity. The capacity increase brought by A_{eff} increase is the rate of capacity increment compared to the 6-core or 8-core fibre that has the smallest A_{eff}. Here the capacity is calculated with SNR_0 for eliminating the XT influence.

Optics EXPRESS

As for 6-core fibres, the A_{eff} increases up to 30.54% for CL-band fibre and 12.51% for SCL-band fibre illustrated in Fig. 8(a). It leads to up to 6.10% capacity increase for 1000 km and up to 23.14% increase for 10000 km. The A_{eff} increase has about four times benefit for 10000 km compared to 1000 km case. Meanwhile, the SCL-band fibre benefits the same as the CL-band fibre with half the A_{eff} increase. In 8-core case in Fig. 8(b), the highest A_{eff} increase is 8.33% smaller than that in 6-core case. The corresponding capacity increase is 4.81% and 16.60% for 1000 km and 10000 km respectively. The ratio between capacity increase and A_{eff} increase are similar in both cases.

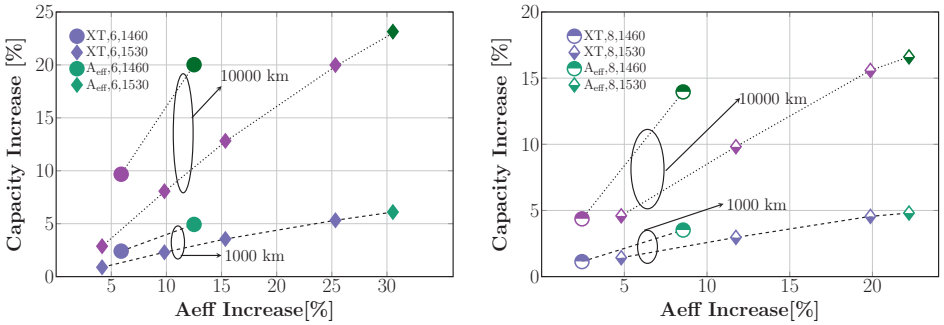

(a) (b)

Fig. 8. Capacity increases with A_{eff} increase:(a) 6-core fibres; (b) 8-core fibres.

Since the XT is included in the SNR calculation as noise in Eq. (1) , by comparing the capacity calculated with SNR_0 and SNR, the capacity penalty induced by the XT noise can be calculated.

$$C(SNR) = \sum_{j}^{N_c} \sum_{i}^{N} B_{ch} \cdot log_2(1 + SNR_i), \tag{2}$$

$$Penalty = \frac{C(SNR_0) - C(SNR)}{C(SNR_0)}, \tag{3}$$

in which N_c is the number of cores in the MCF, N is the total number of wavelength channels in each core and B_{ch} is the bandwidth of each channel.

As illustrated in Fig. 9, the XT-induced penalty increases super-linearly with the XT. For 6-core fibres of which the XT is below −80 dB/km, the capacity penalty is ultra-low and close to zeros in both 1000 km and 10000 km transmission. The marks with darker color are the results at 10000 km. Those 6-core fibres obtained in A_{eff}-optimisation have XT close to −60 dB/km and the influence due to XT starts to show up but stays below 10%. The CL-band fibres suffers more penalty than the SCL-band fibres because the XT is smaller at short wavelength. At S band, with the shorter wavelength, the XT becomes smaller. Thus, it brings less penalty than in the CL bands. When the transmission length increases from 1000 km to 10000 km, XT would be 10 dB higher which leads to double capacity penalty.

Since we are checking the capacity at 1000 km and 10000 km, the MCFs which have XT higher than −30 dB/km and −40 dB/km are not suitable. Thus, in Fig. 9(b), only part of the 8-core fibres are illustrated. 8-core fibres have higher XT and therefore the penalty is up to 14.15% for 1000 km while it is up to 23.01% for 10000 km. Here it can be seen that the penalty increase due to the longer transmission length becomes higher with increasing XT.

Among the 6-core fibres, the penalty induced by XT is much lower than the benefit from the A_{eff} increase. Thus, large-A_{eff} 6-core fibre has better transmission performance. On the other

Optics EXPRESS

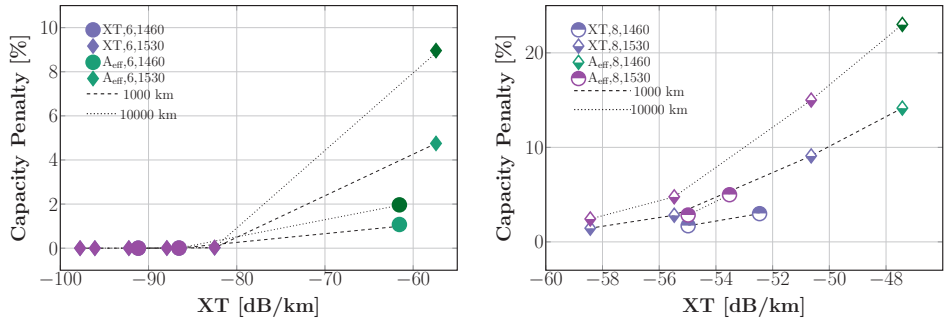

Fig. 9. The XT-induced capacity penalty as a function of the XT at 1550 nm: (a) 6-core fibres; (b) 8-core fibres.

hand, for 8-core fibres, the XT-induced capacity penalty is slightly higher than the capacity increase brought by the A_{eff} increase. Therefore, the 8-core fibres with smaller XT have better capacity.

5. Conclusions

6-core and 8-core fibres covering CL- and SCL-band are designed by the AI-based automated method with a cut-off wavelength regressor for trench-assisted fibre core. The MCF designs benefit nine orders of magnitude reduction of the permutation evaluation compared to the brute force method. 6-core fibres' inter-core crosstalk at 1550 nm is ultra-low between −91.16 and −57.41 dB/km. The XT of 8-core fibres is optimised to −58.43 dB/km for CL band and −54.98 dB/km for SCL band. Following the core profiles generated by our AI-based method, we can conclude that the range width of most of the fibre index profile parameters can be reduced so that the total permutation number can be reduced by 991× for 6-core case and 3.6e5× for 8-core case. This can largely reduce the MCF design time.

In terms of transmission, the capacity of the proposed 8-core fibre is higher than the 6-core fibre covering the same bands from 50 km until 10000 km. The AI-design method delivers a 8-core fibre design that can offer notable capacity improvement, around 32% (approaching the theoretical 33.3%) for 50 km transmission. However, the 8-core fibre has a higher capacity degradation rate over distance leading to similar performance at 10000 km.

Thorough exploration of the effects of bandwidth, XT and A_{eff} is conducted. Increasing the core density from 6 cores to 8 cores in standard cladding diameter reduces bandwidth achieved per core, reduces the A_{eff} and increases the XT. By investigating the spectral spatial efficiency (SSE) of MCFs, it can be noted that 8-core ultra-wide-band fibres experience slightly sharper SSE degradation compared to 6-core ones. The capacity reduction brought by the smaller A_{eff} is similar for both the 6-core and 8-core fibres. However, the change of XT leads to a significantly different performance behaviour over distance. The 6-core fibres have ultra-low XT, that leads to a marginal influence. Minimizing XT in 8-core fibres is more important than offering high A_{eff} as it compensates the capacity penalty imposed by unavoidable A_{eff} reduction within a fixed cross sectional area.

Optics EXPRESS

Appendix A. Cut-off wavelength regressor

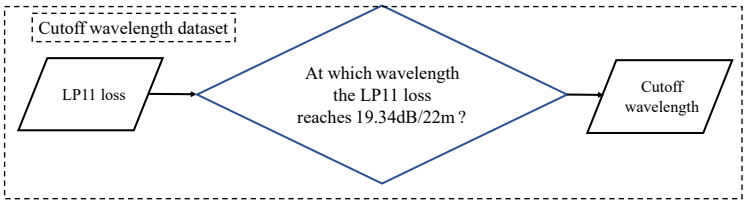

(a)

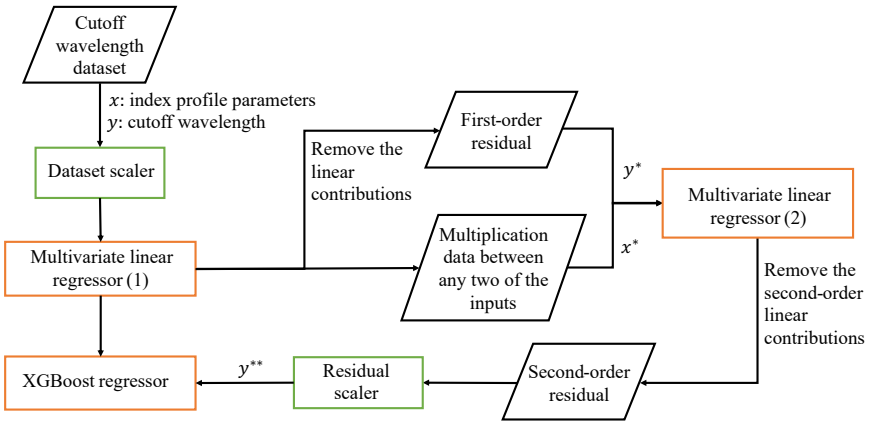

(b)

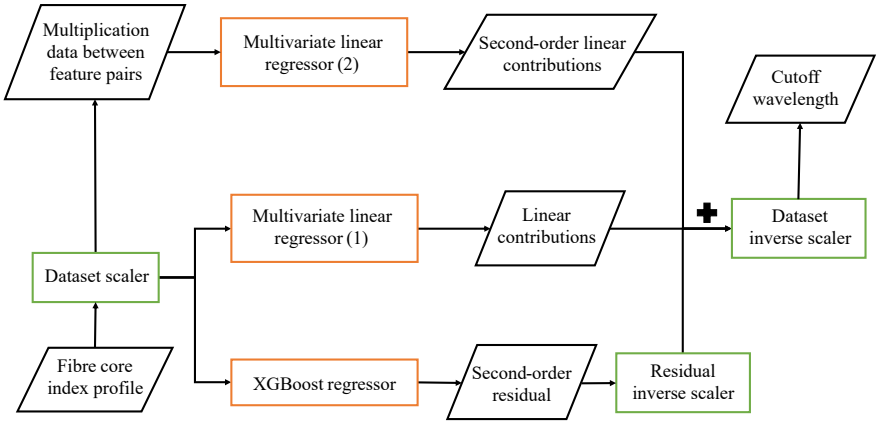

(c)

Fig. 10. (a) workflow to create cut-off wavelength dataset; (b) workflow to train cut-off wavelength regressors; (c) workflow to predict cut-off wavelength for one fibre structure.

Appendix B. Attenuation and noise figure modelling

Optical fibre attenuation has several attributions: Rayleigh scattering, absorption due to the OH^- ion, waveguide imperfection, infrared absorption and ultra-violate absorption. In [21], the attenuation of SMF is modelled. Among them the Rayleigh scattering is the most weighted. To

Optics EXPRESS

model the Rayleigh scattering of our silica-based trench-assisted fibre core, we take the dopant concentration and optical power distribution into consideration [22] and calculate the Rayleigh scattering coefficient. Since Rayleigh scattering is proportional to $1/\lambda^4$, we can model it over the whole bandwidth of the fibre core. The absorption due to the OH^- ion is ignored because we assume that the fibre is dry. Waveguide imperfections lead to losses with a constant value shown as the Eq. (3) in [21]. As for the infrared and ultra-violate absorption, the fitting function Eq. (5) and Eq. (6) in [21] of the SSMF are used.

The attenuation curves of the SSMF and MCFs are illustrated in Fig. 11. The MCFs' attenuation is higher than that of the SSMF because of the higher core index as shown in Fig. 5. Similarly, the 6-cpre fibres have slightly higher attenuation than the 8-core fibres.

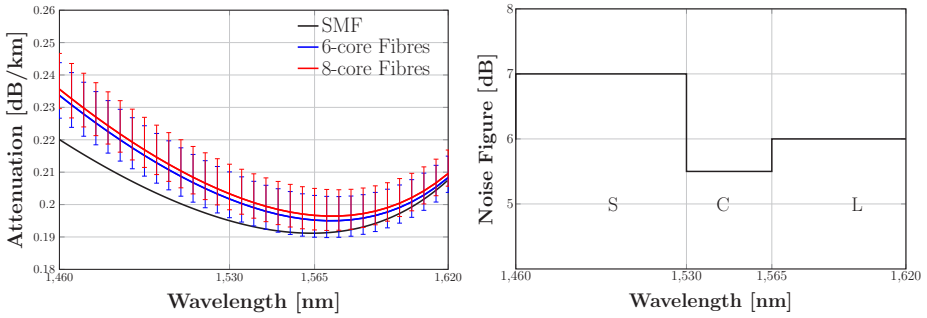

(a) (b)

Fig. 11. The assumption of attenuation (a) and noise figure (b).

Appendix C. SNR

In each design case, we pick the fibre which provides the best transmission performance. The fibre properties of the fibres—n_{eff}, A_{eff} and chromatic dispersion—are shown in Table 2.

Table 2. The n_{eff}, A_{eff} and chromatic dispersion (CD) at 1550 nm for 8-core fibre design shown in Fig. 6

Case name	Constrains	n_{eff} core1/core2	A_{eff} [μm^2] core1/core2	CD [ps/km/nm] core1/core2
6core-CL	XT-optimisation [70 80]	1.44695/1.44782	71.12/70.07	23.84/23.52
6core-SCL	A_{eff}-optimisation	1.44707/1.44707	64.41/64.41	23.51/23.51
8core-CL	XT-optimisation [55 65]	1.44738/1.44888	57.26/56.42	23.05/23.16
8core-SCL	XT-optimisation [55 65]	1.44726/1.44838	57.69/55.96	23.07/23.00

There are several factors influencing the SNR performance. Here we show them separately in Fig. 12. The transceiver noise (TRX) is assumed to be 23 dB. The XT, amplified spontaneous emission (ASE) and nonlinear interference (NLI) increase with the transmission length. The XT is worse for the longer wavelength and thus, the gap between the SNR without XT and SNR becomes wider with the increasing wavelength.

Optics EXPRESS

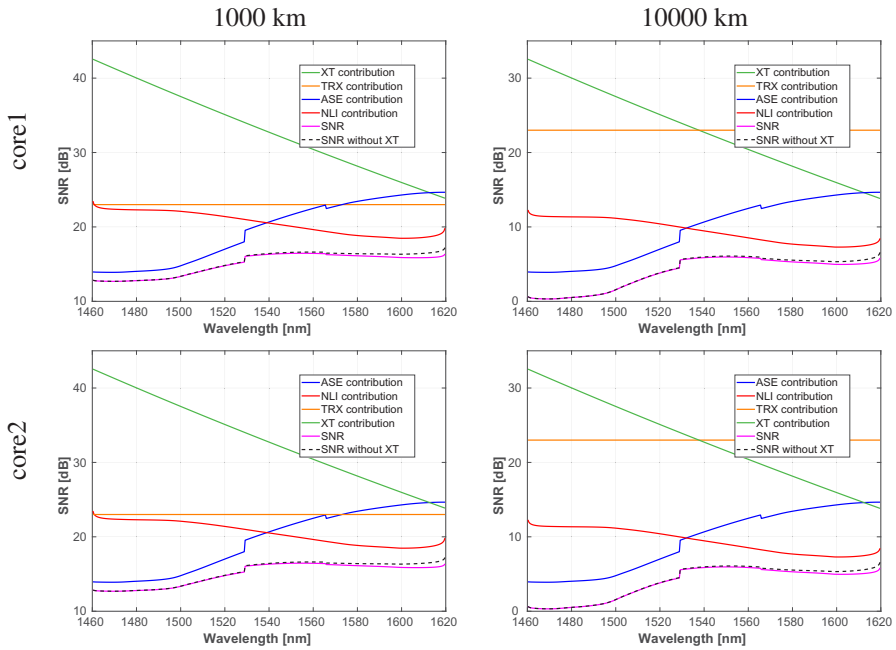

Fig. 12. SNR and its contributions including XT, transceiver (TRX), amplified spontaneous emission (ASE) and nonlinear interference (NLI) of two types of cores in SCL-band 6-core fibre.

Appendix D. PSO workflow

The workflow of the PSO-based fibre design process is illustrated in Fig. 13. Based on the fitness values, the global best particle (gbest) and the personal best particle (pbest) can be picked for each generation of particles. They are included in the velocity update and then the velocity determines the particles moving path. After a certain number of generations, when the convergence condition is met, the optimisation is finished. If all the constraints are satisfied, the transmission performance of the MCF will be evaluated.

Optics EXPRESS

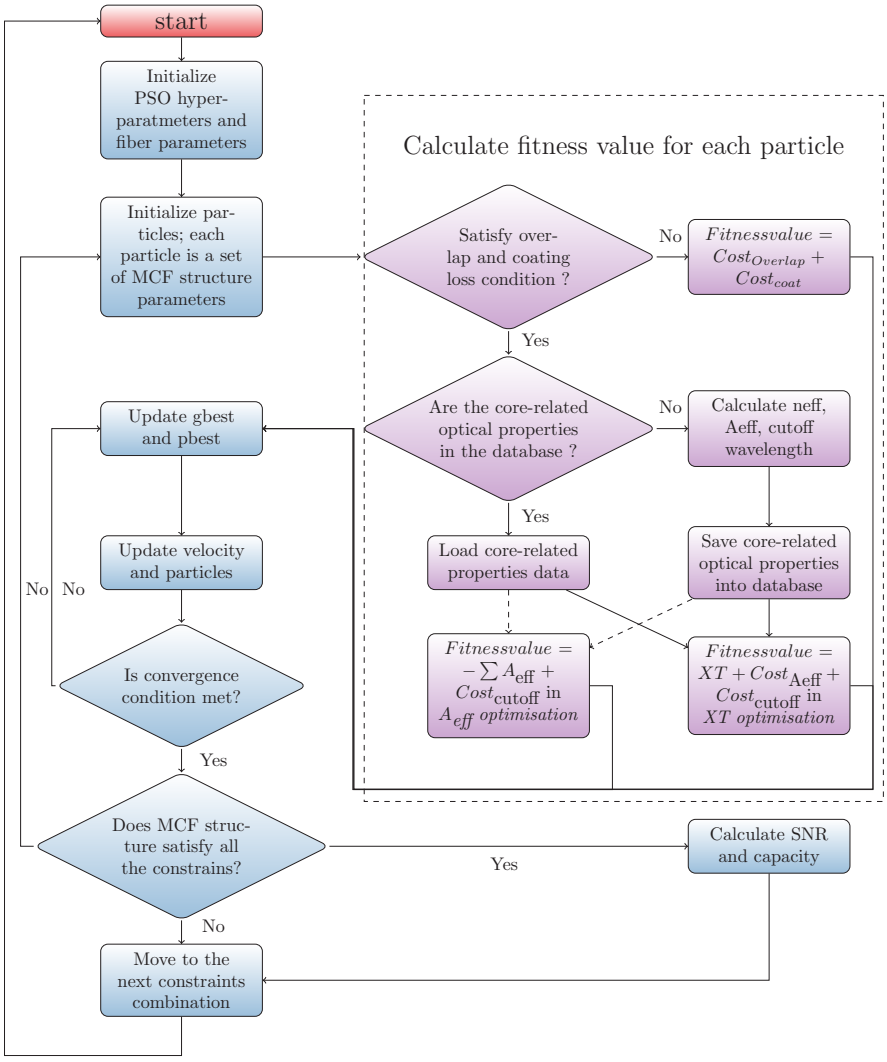

Fig. 13. Workflow of MCF optimisation process with PSO.

Optics EXPRESS

Funding. UK Research and Innovation Future Leaders Fellowship (MR/T041218/1); Engineering and Physical Sciences Research Council (EP/L015455/1, EP/R035342/1, EP/T026081/1).

Disclosures. The authors declare no conflicts of interest.

Data availability. Data underlying the results presented in this paper are not publicly available at this time but may be obtained from the authors upon reasonable request.

References

1. Y. Sagae, T. Matsui, T. Sakamoto, and K. Nakajima, "Ultra-low crosstalk multi-core fiber with standard 125-μm cladding diameter for 10, 000km-class long-haul transmission," IEICE Trans. Commun. **E103.B**(11), 1199–1205 (2020).
2. B. J. Puttnam, R. S. Luís, G. Rademacher, Y. Awaji, and H. Furukawa, "319 tb/s transmission over 3001 km with s, c and l band signals over >120nm bandwidth in 125 μm wide 4-core fiber," in *Proc. of Opt. Fiber Commun. Conf. and Exhib. (OFC)*, (2021), pp. 1–3.
3. T. Hayashi, T. Nakanishi, K. Hirashima, O. Shimakawa, F. Sato, K. Koyama, A. Furuya, Y. Murakami, and T. Sasaki, "125-μm-cladding eight-core multi-core fiber realizing ultra-high-density cable suitable for o-band short-reach optical interconnects," J. Lightwave Technol. **34**(1), 85–92 (2016).
4. Y. Wang, T. Fujisawa, T. Sakamoto, T. Matsui, K. Nakajima, and K. Saitoh, "Step index 8-core fiber with 125-μm cladding diameter for o-band use," in *Proc. of Opto. Commun. Conf. (OECC)*, (2020), pp. 1–3.
5. S. Jiang, L. Ma, M. N. Velazquez, Z. He, and J. K. Sahu, "Design of 125-μm cladding diameter multi core fibers with high core multiplexing factor for wide band optical transmission," Opt. Fiber Technol. **50**, 55–61 (2019).
6. Y. Wang, T. Fujisawa, Y. Sagae, T. Sakamoto, T. Matsui, K. Nakajima, and K. Saitoh, "A novel core allocation in heterogeneous step-index multi-core fibers with standard cladding diameter," J. Lightwave Technol. **39**(22), 7231–7237 (2021).
7. T. Hayashi, T. Taru, O. Shimakawa, T. Sasaki, and E. Sasaoka, "Characterization of crosstalk in ultra-low-crosstalk multi-core fiber," Opt. Express **30**(4), 583–589 (2012).
8. X. Mu, F. M. Ferreira, A. Ottino, and G. Zervas, "Design optimization of uncoupled six-core fibers in standard cladding diameter using artificial intelligence," in *Proc. of Opt. Fiber Commun. Conf. and Exhib. (OFC)*, (2021), p. Th1A.34.
9. J. Tu, K. Saitoh, M. Koshiba, K. Takenaga, and S. Matsuo, "Design and analysis of large-effective-area heterogeneous trench-assisted multi-core fiber," Opt. Express **20**(14), 15157–15170 (2012).
10. J. Tu, K. Saitoh, K. Takenaga, and S. Matsuo, "Heterogeneous trench-assisted few-mode multi-core fiber with low differential mode delay," Opt. Express **22**(4), 4329–4341 (2014).
11. L. A. de Montmorillon, M. Bigot Astruc, and P. Sillard, "Cutoff mechanisms in bend-insensitive single-mode fibers," in *Proc. of Opt. Fiber Commun. Conf. and Exhib. (OFC)*, (2011), p. OTuA1.
12. M. Koshiba, K. Saitoh, and Y. Kokubun, "Heterogeneous multi-core fibers: proposal and design principle," IEICE Electron. Express **6**(2), 98–103 (2009).
13. D. Semrau, L. Galdino, E. Sillekens, D. Lavery, R. I. Killey, and P. Bayvel, "Modulation format dependent, closed-form formula for estimating nonlinear interference in s+c+l band systems," in *Proc. of Eur. Conf. Opt. Commun. (ECOC)*, (2019), p. W.1.D.
14. K. Takenaga, Y. Arakawa, Y. Sasaki, S. Tanigawa, S. Matsuo, K. Saitoh, and M. Koshiba, "A large effective area multi-core fiber with an optimized cladding thickness," Opt. Express **19**(26), B543–B550 (2011).
15. X. Mu, A. Ottino, F. M. Ferreira, and G. Zervas, "Optimization of 125-μm heterogeneous multi-core fibre design using artificial intelligence," IEEE J. Sel. Topics Quantum Electron. **28**(4), 1–13 (2022).
16. T. Sakamoto, K. Saitoh, N. Hanzawa, K. Tsujikawa, L. Ma, M. Koshiba, and F. Yamamoto, "Crosstalk suppressed hole-assisted 6-core fiber with cladding diameter of 125 μm," in *Proc. of Eur. Conf. Opt. Commun. (ECOC)*, (2013), p. Mo.3.A.3.
17. K. Takenaga, Y. Arakawa, S. Tanigawa, N. Guan, S. Matsuo, K. Saitoh, and M. Koshiba, "Reduction of crosstalk by trench-assisted multi-core fiber," in *Proc. of Opt. Fiber Commun. Conf. and Exhib. (OFC)*, (2011), p. OWJ4.
18. T. Gonda, K. Imamura, R. Sugizaki, Y. Kawaguchi, and T. Tsuritani, "125 μm 5-core fibre with heterogeneous design suitable for migration from single-core system to multi-core system," in *Proc. of Eur. Conf. Opt. Commun. (ECOC)*, (2016), p. W.2.B.1.
19. R. S. Luís, G. Rademacher, B. J. Puttnam, D. Semrau, R. I. Killey, P. Bayvel, Y. Awaji, and H. Furukawa, "Crosstalk impact on the performance of wideband multicore-fiber transmission systems," IEEE J. Sel. Topics Quantum Electron. **26**(4), 1–9 (2020).
20. G. M. Saridis, D. Alexandropoulos, G. Zervas, and D. Simeonidou, "Survey and evaluation of space division multiplexing: From technologies to optical networks," IEEE Commun. Surv. Tutorials **17**(4), 2136–2156 (2015).
21. M. Fugihara and A. N. Pinto, "Attenuation fitting function," Microw. Opt. Technol. Lett. **51**(10), 2294–2296 (2009).
22. K. Tsujikawa, K. Tajima, K. Shiraki, and I. Sankawa, "Method for predicting rayleigh scattering loss of silica-based optical fibers," J. Lightwave Technol. **25**(8), 2122–2128 (2007).